Microbial carbohydrate depolymerization by antigen-presenting cells: Deamination prior to presentation by the MHCII pathway

Jinyou Duan, Fikri Y. Avci, and Dennis L. Kasper*

Department of Medicine, Channing Laboratory, Brigham and Women's Hospital and Department of Microbiology and Molecular Genetics, Harvard Medical School, Boston, MA 02115

Communicated by John B. Robbins, National Institutes of Health, Bethesda, MD, February 1, 2008 (received for review October 4, 2007)

After uptake by the endosome of an antigen-presenting cell (APC), exogenous proteins are known to be degraded into peptides by protease digestion. Here, we report the mechanism by which pure carbohydrates can be depolymerized within APC endosomes/lysosomes by nitric oxide (NO)-derived reactive nitrogen species (RNSs) and/or superoxide-derived reactive oxygen species (ROSs). Earlier studies showed that depolymerization of polysaccharide A (PSA) from *Bacteroides fragilis* in the endosome depends on the APC's having an intact inducible nitric oxide synthase (iNOS) gene; the chemical mechanism underlying depolymerization of a carbohydrate within the endosome/lysosome is described here. Examining the ability of the major RNSs to degrade PSA, we determined that deamination is the predominant mechanism for PSA processing in APCs and is a required step in PSA presentation to CD4$^+$ T cells by MHCII molecules. Structural characterization of the NO-derived product PSA-NO indicates that partial deaminative depolymerization does not alter the zwitterionic nature of PSA. Unlike native PSA, PSA-NO is presented by iNOS-deficient APCs to induce CD4$^+$ T cell proliferation. Furthermore, metabolically active APCs are required for PSA-NO presentation. In contrast to PSA degradation by RNSs, dextran depolymerization in the endosome depends on ROSs, including hydrogen peroxide- and superoxide-derived ROSs. This study provides evidence that MHCII pathway-mediated carbohydrate antigen processing in APCs is achieved by chemical reactions. RNSs and ROSs may be involved in the presentation of glycopeptides by MHC molecules via the processing of other carbohydrate-containing antigens, such as bacterial or viral glycoproteins or glycoconjugate vaccines.

antigen processing | MHC class II | reactive nitrogen species

Carbohydrates are increasingly recognized as key mediators of immune reactions (1, 2). Capsular polysaccharides expressed on the surface of many pathogenic bacteria are carbohydrates traditionally thought to stimulate an immune response that, in all cases, was assumed to be T cell independent (3). However, our earlier studies showed that polysaccharides with a zwitterionic charge motif can indeed activate CD4$^+$ T cells after processing and presentation through the MHCII pathway (1). Information has been lacking on the chemical mechanism(s) underlying this processing.

In terms of T cell activation, polysaccharide A (PSA) [its structure as shown in supporting information (SI) Fig. S1], the major zwitterionic polysaccharide (ZPS) from *Bacteroides fragilis* and the best characterized ZPS (4, 5), has profound biological importance. During intestinal colonization in mice, PSA-expressing *B. fragilis* directs maturation of the mammalian immune system. Mono-association of germ-free mice with a WT PSA-bearing *B. fragilis* strain—but not with an isogenic mutant incapable of synthesizing PSA—corrects systemic T cell deficiencies, redresses Th1/Th2 imbalances, and directs lymphoid organogenesis (5). Toll-like receptor 2 (TLR2) coordinates an innate and adaptive immune response to PSA (a TLR2 agonist) that results in production of IFN γ—a key factor in the Th1 differentiation observed in colonization studies (6).

Once within the APC endosomes/lysosomes, PSA is degraded to a smaller molecule (≈10–15 kDa) before being presented to CD4$^+$ T cells (1). The surprising dependence of this degradation on inducible nitric oxide synthase (iNOS) suggests a processing mechanism distinct from the enzymatic cleavage responsible for cellular processing of protein antigens. Given the established importance of PSA and the lack of information on processing of this ZPS or any other carbohydrate, we sought to define the chemical mechanism(s) responsible for PSA processing. An in-depth understanding of this key process may elucidate non-enzymatic processing of numerous antigens through this pathway.

Results

Degradation of Carbohydrates Within APC Endosomes by Reactive Nitrogen Species (RNSs) and Reactive Oxygen Species (ROSs). After exposure of APCs to cytokines or microbial products, iNOS is up-regulated and generates large quantities of nitric oxide (NO) by catalyzing the oxidation of L-arginine (7). NO is a short-lived radical that forms various NO-derived RNSs. To delineate the mechanism of NO-dependent processing of PSA in APCs, we identified the role of iNOS in the processing of PSA in CD11c+ dendritic cells (DCs). It had been shown that iNOS is required for PSA processing by total splenic mononuclear cells, but no work had been performed on processing specifically in DCs, the most relevant APCs for presenting PSA to T cells.

After 72 h of uptake and processing, PSA is degraded to a different extent in WT and in iNOS$^{-/-}$ DCs (Fig. 1*A*), and *N*-acetyl PSA (the fully *N*-acetylated product of PSA) is degraded equally in both WT and iNOS$^{-/-}$ DCs (Fig. 1*B*). Because, in response to external stimuli, ROSs and RNSs produce synergistic and/or antagonistic effects in APCs (8), these data suggest that, in addition to RNSs, other reactive species (for instance, ROSs) in APCs may effectively process polysaccharides with a zwitterionic charge (PSA) or a negative charge (*N*-acetyl PSA). Furthermore, the substantially greater suppression of PSA degradation in iNOS$^{-/-}$ DCs than in WT DCs (Fig. 1*A*) indicates that RNSs are the predominant reactive species responsible for PSA processing. However, *N*-acetyl PSA processing in WT DCs does not differ significantly from that in iNOS$^{-/-}$ DCs (Fig. 1*B*). Because deaminative depolymerization at free amino or *N*-sulfo groups—but not at *N*-acetyl groups—of

Author contributions: J.D., F.Y.A., and D.L.K. designed research; J.D. and F.Y.A. performed research; J.D., F.Y.A., and D.L.K. contributed new reagents/analytic tools; J.D., F.Y.A., and D.L.K. analyzed data; and J.D., F.Y.A., and D.L.K. wrote the paper.

The authors declare no conflict of interest.

*To whom correspondence should be addressed. E-mail: dennis_kasper@hms.harvard.edu.

This article contains supporting information online at www.pnas.org/cgi/data0800974105/DCSupplemental.

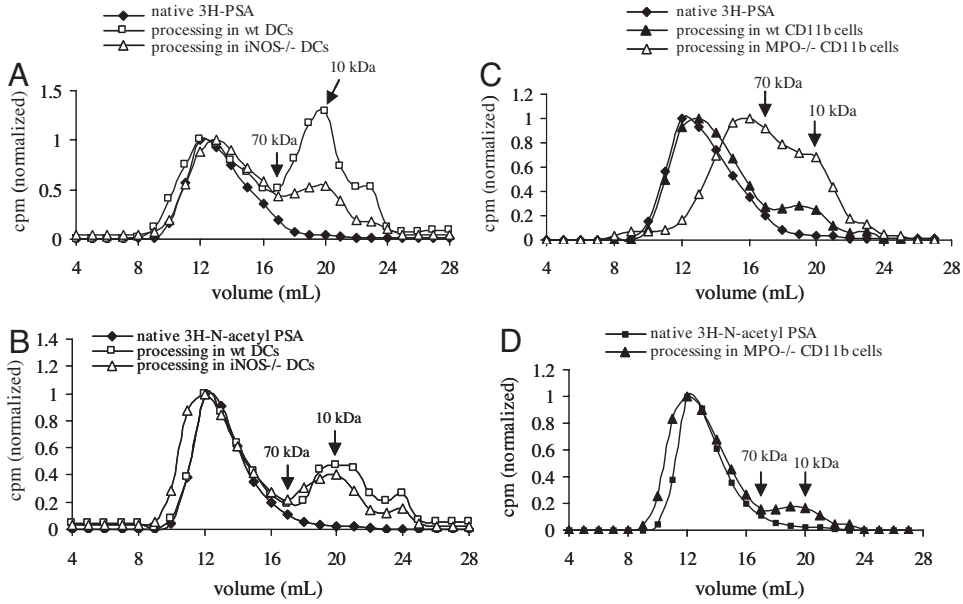

Fig. 1. Gel permeation chromatography of the degradation of ^{3}H-PSA or ^{3}H-*N*-acetyl PSA in mouse APCs. The degradation of PSA and *N*-acetyl PSA recovered from DC lysates represents both endosomal and cell surface-associated bacterial polysaccharide. ^{3}H-PSA or ^{3}H-*N*-acetyl PSA was incubated with CD11c+ DCs from WT or iNOS$^{-/-}$ mice ($n = 3$) (*A* and *B*) or with CD11b+ monocytes/macrophages from WT or MPO$^{-/-}$ mic ($n = 2$)e (*C* and *D*). Native ^{3}H-PSA, ^{3}H-*N*-acetyl PSA, and their products recovered by lysis of DCs or monocytes/macrophages were analyzed by FPLC (Superose 12), and fractions were assayed for radioactivity to determine the size of the polysaccharide eluting from the column.

amino sugars of glycosaminoglycans (9, 10) has been well described, we concluded that RNS-mediated processing of PSA occurs through a deamination reaction.

Release of NO in monocytes/macrophages (but not DCs) is strictly controlled by myeloperoxidase (MPO), which serves as a gatekeeper. Therefore, in MPO$^{-/-}$ monocytes/macrophages, large amounts of NO are generated (11). PSA is degraded more in MPO$^{-/-}$ CD11b+ cells than in WT CD11b+ cells (Fig. 1*C*). RNSs react with superoxide (the precursor of ROSs in phagocytic cells) to form peroxynitrite (12), which (as shown below) has no effect on PSA depolymerization. Because MPO$^{-/-}$ macrophages have an excess of NO that suppresses any effect of ROSs on PSA degradation, this degradation results primarily from RNSs. Furthermore, in MPO$^{-/-}$ CD11b+ cells, processing of *N*-acetyl PSA is significantly reduced (Fig. 1*D*) from that of native PSA; this finding again indicates that deamination is the most important chemical reaction of RNSs during PSA processing and suggests that ROSs are primarily responsible for processing *N*-acetyl PSA.

Like carbohydrates with zwitterionic charges (PSA) or negative charges (*N*-acetyl PSA), neutral carbohydrates (e.g., dextran) are degraded within the APC endosome/lysosome. After uptake by APCs, dextran is significantly degraded to a smaller molecular size (Fig. S2). Degradation is partially suppressed by the superoxide scavenger MnTBAP or the hydroperoxide scavenger pyruvate but not by the hydroxyl radical scavenger D-mannitol. Taken together, these data indicate that carbohydrates can be depolymerized within the APC endosome/lysosome by RNSs and/or ROSs by chemical mechanisms that vary with the fine structure of the polysaccharide polymer.

Identification of RNSs Degrading PSA. We next asked which RNSs can chemically degrade PSA. Thus far, only NO, nitrous acid, *S*-nitrosothiols, and peroxynitrite have been shown to be capable of degrading carbohydrate polymers (9, 10, 12). Specifically, these RNSs degrade heparin, heparan sulfate, and chondroitin sulfate through a common deaminative mechanism (9, 10). In contrast, peroxynitrite selectively degrades hyaluronic acid and chondroitin sulfate but not heparin (12) and degrades carbohydrate polymers via an unidentified mechanism thought to resemble chemical depolymerization by free hydroxyl radical attack. We investigated whether NO itself and/or peroxynitrite can degrade PSA.

A 1:3 dilution of NO-saturated solution significantly degrades PSA at neutral pH (Fig. S3*A*). In contrast, *N*-acetyl PSA, which contains no free amino groups, is completely resistant to NO attack (Fig. S3*B*), a result suggesting that NO degrades PSA through a deaminative mechanism. We converted NO into nitrogen dioxide with carboxyl-PTIO (carboxyl-2-[4-carboxyphenyl]-4,4,5,5-tetramethylimidazoline-l-oxyl-3-oxide) to diminish the NO available for PSA degradation. This chemical reaction generates products with greater molecular size than those seen without carboxyl-PTIO treatment (Fig. S3*A*). The incomplete inhibition of the NO attack on PSA by carboxyl-PTIO is probably due to either the presence of NO remnants or the formation of another deaminative reagent, nitrous acid.

We compared the effect of peroxynitrite and hydroxyl radical—because both can depolymerize hyaluronan and chondroitin sulfate (9, 12)—on the molecular size of PSA. PSA is susceptible to degradation by the hydroxyl radical generated during autooxidation of ferrous cation (13), and this susceptibility is greatly suppressed by the hydroxyl radical scavenger D-mannitol (Fig. S3*C*). In contrast, at neutral pH, 3 mM 3-morpholinosydnonimine hydrochloride (SIN-1), the peroxynitrite generator, does not reduce the molecular size of PSA. As a positive control, we degraded hyaluronic acid slightly with 3 mM SIN-1 (Fig. S4). Like PSA under the same conditions, *N*-acetyl PSA was resistant to peroxynitrite attack (data not shown). Thus, the zwitterionic charge motif of PSA did not account for the molecule's protection from peroxynitrite attack.

To date, the interaction between nitroxyl and carbohydrates has not been explored, although nitroxyl is reportedly more toxic to (or reactive with) cells than is NO itself (14). *In vitro*, nitroxyl can be generated by protonation of Angeli's salt (sodium trioxodinitrate) (15). As shown in Fig. S3 and Fig. S5, mM Angeli's salt slightly reduces the molecular size of PSA in the presence or

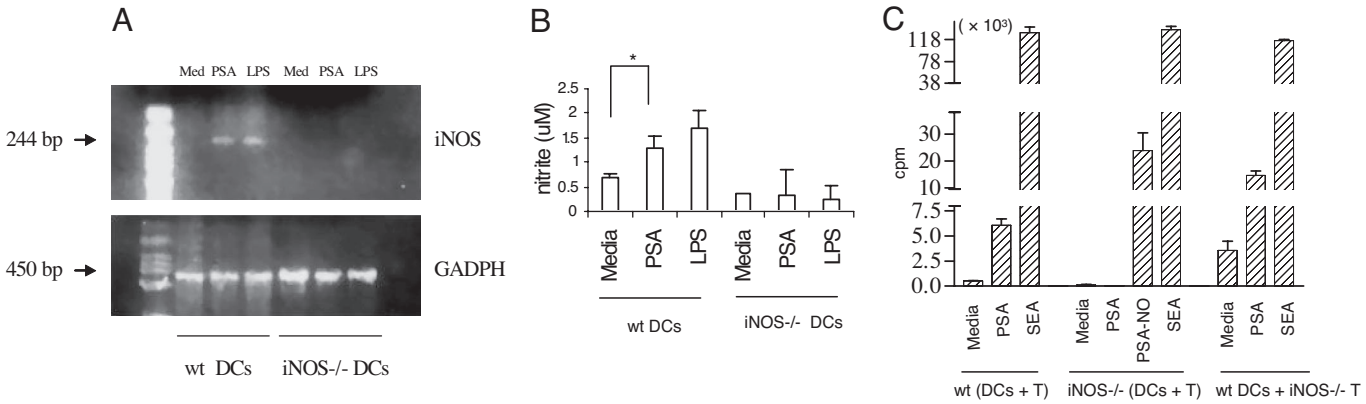

Fig. 2. iNOS in mouse APCs is necessary for intact PSA—but not for PSA-NO—to induce CD4$^+$ T cell activation *in vitro* and abscess formation *in vivo*. (*A*) After stimulation with PSA or LPS for 18 h, iNOS mRNA expression was identified in WT but not in iNOS$^{-/-}$ DCs ($n = 3$). (*B*) After stimulation of DCs with PSA or LPS for 72 h, nitrite production in cell supernatants was determined. Data are mean ± SD values. *, $P < 0.04$ ($n = 3$). (*C*) PSA, PSA-NO, or control SEA was added to cocultures of DCs and CD4$^+$ T cells from either WT or iNOS$^{-/-}$ mice. Key for cell combinations tested: WT (DCs + T), DCs and CD4$^+$ T cells from WT mice; iNOS$^{-/-}$ (DCs + T), DCs and CD4$^+$ T cells from iNOS$^{-/-}$ mice; and WT DCs + iNOS$^{-/-}$ T, DCs from WT mice and CD4$^+$ T cells from iNOS$^{-/-}$ mice ($n = 3$).

absence of oxygen. However, treatment with 3 mM Angeli's salt does not affect *N*-acetyl PSA. Because nitroxyl can be converted into NO through metal-mediated oxidation or by direct reaction with oxygen (15), nitroxyl-induced degradation of PSA is probably achieved through deamination.

In the Absence of iNOS, the Deaminative Product PSA-NO—but Not Native PSA—Activates T Cells *in Vitro* and *in Vivo*. RT-PCR analyses revealed that PSA induces iNOS mRNA expression in WT DCs but not in iNOS$^{-/-}$ DCs. Furthermore, up-regulation of iNOS gene transcription in DCs correlates with NO radical production (Fig. 2 *A* and *B*). This observation is consistent with our previous findings in other APCs (macrophages) (6). *In vitro*, native PSA induces T cell proliferation in cocultured CD4$^+$ T cells and DCs from the spleens of WT mice (Fig. 2*C*) but not in cocultured cells from the spleens of iNOS$^{-/-}$ mice. CD4$^+$ T cells deficient in iNOS do proliferate when PSA-NO (a NO-derived product of PSA, molecular mass = ≈16 kDa, see *Materials and Methods*) is cocultured with iNOS$^{-/-}$ DCs. Because T cells from WT and iNOS$^{-/-}$ mice differ in terms of cell death and immune memory (16), we tested whether PSA activates iNOS$^{-/-}$ T cells when WT DCs are used as APCs. If iNOS$^{-/-}$ DCs are replaced by WT DCs, native PSA does activate iNOS$^{-/-}$ T cells—a result demonstrating that the failure of PSA to activate T cells from iNOS$^{-/-}$ mice is attributable to iNOS deficiency in APCs rather than T cells. The requirement for iNOS in activation of T cells by native PSA but not by PSA-NO supports our report that iNOS is essential for processing of intact PSA (1). These *in vitro* data provide a solid immunological basis for the finding *in vivo* that both intact PSA and PSA-NO induce abscess formation in WT mice, a model that requires activation of T cells by ZPSs (17). In contrast, intact PSA (but not PSA-NO) fails to facilitate abscess formation in iNOS$^{-/-}$ mice (Table 1).

Table 1. Abscess formation induced by PSA or PSA-NO in WT or iNOS$^{-/-}$ mice

Group	Strain	Challenge*	No. of animals with abscess/total (%)	$P^\dagger$
A	C57BL/6J	PBS	1/8 (12.5)	
B		PSA	7/8 (87.5)	0.01
C		PSA-NO	6/8 (75)	0.04
D	B6129P2-Nos2P^{tm1LauP}/J	PSA	2/8 (25)	NS
E		PSA-NO	7/8 (87.5)	0.01

*Inocula were given via the i.p. route with SCC.
†Compared with PBS control ($n = 2$).

PSA-NO Activates T Cells Through the MHCII Pathway. PSA-NO induces human CD4$^+$ T cell proliferation at concentrations of 100, 10, and 1 μg/ml (Fig. S6). Interestingly, PSA-NO is more active than native PSA on a stoichiometric basis and elicits the strongest T cell proliferative responses at 1 μg/ml among the doses tested.

Both colchicine (which blocks microtubule polymerization) and brefeldin A (which blocks trafficking between the Golgi apparatus and the endoplasmic reticulum) effectively inhibit PSA-induced activation of human CD4$^+$ T cells (Fig. 3*A*). Furthermore, PSA-NO presentation to T cells by human APCs depends on the MHCII HLA-DR molecule but not on the MHCII HLA-DP and HLA-DQ molecules or the MHCI molecules HLA-A, -B, and -C and their isotype controls (Fig. 3*B*). In similar blocking experiments in a mouse T cell proliferation assay, colchicine, brefeldin A, and monoclonal antibody (mAb) to I-A/I-E inhibit PSA-NO-induced T cell activation when mouse DCs are used as APCs (Fig. 3*C*). Because the superantigen staphylococcal enterotoxin A (SEA) can bypass antigen trafficking and bind directly to MHC molecules on the surface of an APC, we tested whether fixed APCs can still elicit T cell responses when presented with PSA-NO (Fig. 3*D*). Unlike superantigens, PSA-NO fails to activate T cells after DCs are fixed with formaldehyde (Fig. 3*D*).

Structural Evidence on the Zwitterionic Nature of PSA-NO. The ^{1}H-NMR data for PSA and PSA-NO (Fig. 4) were identical (within the detection limits), suggesting that deamination does not significantly disturb PSA's repeating units except for modification at cleavage sites. We carried out *N*-acetylation of PSA-NO and PSA and used ^{1}H-NMR to observe the incorporation of acetyl groups into these sugars. After *N*-acetylation, in ^{1}H-NMR spectra of both PSA and PSA-NO, we detected incorporation of one *N*-acetyl group per repeating unit of PSA/PSA-NO (three additional hydrogens at 2.17 ppm) corresponding to 4-*N*-acetyl groups of the AAT*p* residues (Fig. 4). In addition, the deoxymethyl peak of the AAT*p* residue (C-6) shifted upfield (0.18 ppm) in both PSA and PSA-NO when N-acetylated, a change clearly demonstrating that it was the 4-amino group of the AAT*p* residue in PSA-NO that remained intact during deamination by NO. Structural characterizations of both PSA-NO and PSA were performed by analyzing their ^{1}H

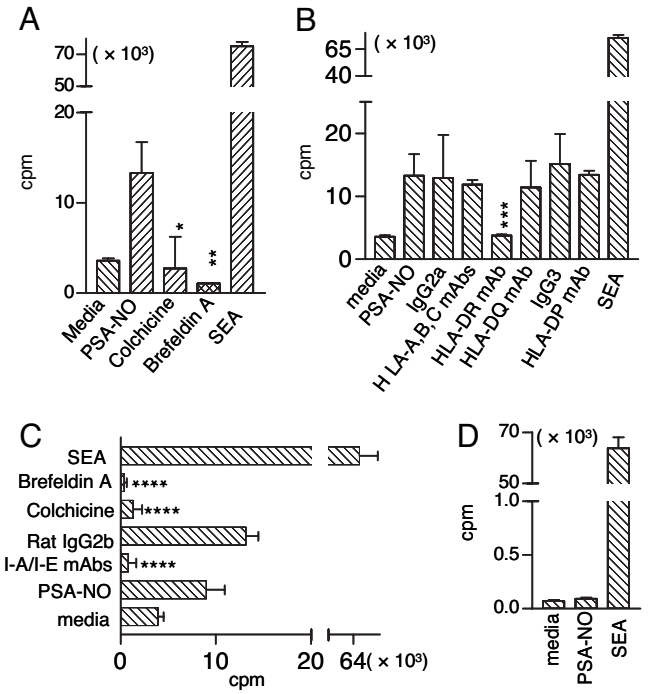

Fig. 3. T cell proliferation induced by the NO-derived product PSA-NO (≈16 kDa) is blocked by inhibitors of the MHCII pathway. (*A–C*) PSA-NO-induced T cell activation was inhibited by colchicine and brefeldin A in both human (*A*) and mouse (*C*) T cell proliferation assays or by mAbs to HLA-DR (*B*) and I-A/I-E (*C*). Error bars indicate SD. *, $P = 0.002$; **, $P = 0.003$; ***, $P = 0.008$; ****, $P < 0.003$. (P values were calculated relative to PSA-NO alone; $n = 3$.) (*D*) Fixation of DCs eliminated PSA-NO-induced T cell proliferation ($n = 3$).

and $^1H-^1H$ NMR (COSY) spectra (Fig. S7); the results matched our original structural elucidation of PSA (4).

Discussion

It is well known that the MHCI and MHCII pathways present proteins or protein conjugates to T cells. In both pathways, protein antigens are processed to peptides by proteases before being loaded onto the MHC molecule and presented. Glycolipids are presented to T cells by the CD1 molecule, either directly or after enzymatic degradation (18). In addition to the general belief that ROSs and RNSs within activated neutrophils and macrophages can destroy ingested microbes, it was recently reported that carbohydrate chains in heparan sulfate-containing proteoglycans are degraded through an NO-dependent mechanism (19). Here, we report that RNS and ROS processing of carbohydrate antigens (or other antigens) into products to be presented to T cells by APCs. Our elucidation of the mechanism of polysaccharide processing by these reactive species extends our understanding of nonprotein antigen processing within the endosome (20).

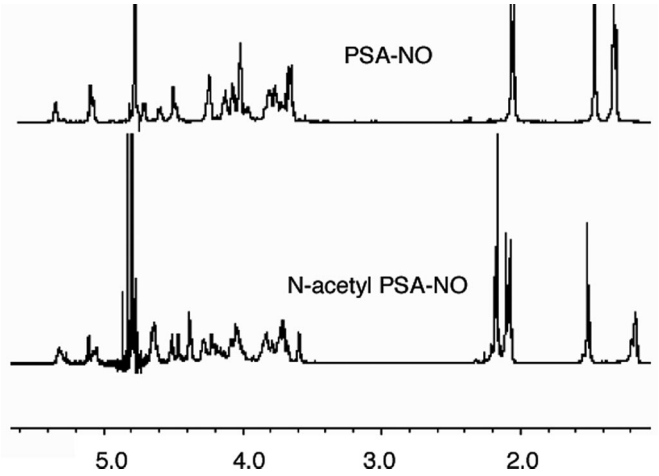

Fig. 4. PSA-NO retains the zwitterionic nature of PSA. Results of ^1H-NMR of PSA-NO and *N*-acetyl PSA-NO are shown. The spectra were recorded at 298 K in deuterium oxide on a Varian VNMRS-600 NMR spectrometer. HOD (4.80 ppm) was used as the chemical-shift reference in NMR experiments.

CD11c+ DCs are the APCs likely to be responsible for PSA presentation during intestinal colonization of animals with *B. fragilis* (5). To characterize the role of iNOS in PSA processing in DCs, we first provided evidence that PSA up-regulates NO production at both the gene and the protein level (Fig. 2 *A* and *B*). This iNOS up-regulation in APCs is probably mediated through the NF-κB signaling pathway resulting from PSA stimulation of TLR2 on the APC surface (6). The essential role of iNOS in DC maturation accounts for differences in expression of MHCII molecules on the surfaces of WT and iNOS$^{-/-}$ DCs (21) and thus may affect the quantity of processed PSA actually presented on the cell surface. To determine the total amount of processed PSA in DCs, we analyzed whole-cell lysates—rather than the endosomal/lysosomal compartment alone—in WT and iNOS$^{-/-}$ DCs (Fig. 1 *A* and *B*). By comparing the molecular sizes of PSA and *N*-acetyl PSA in lysates from these two types of DCs, we determined that RNSs are the major reactive species responsible for processing PSA and that deamination is the chemical reaction involved. Because deamination requires a free amino or *N*-sulfonyl group, we compared PSA with *N*-acetyl PSA, which lacks the free amino group. Our conclusion that deamination is responsible for PSA depolymerization is based on (*i*) greater reduction in processed PSA recovered from WT than from iNOS$^{-/-}$DCs (Fig. 1*A*); (*ii*) less change in processed *N*-acetyl PSA recovered from WT versus iNOS$^{-/-}$ DCs (Fig. 1*B*); (*iii*) drastic reduction in processed PSA recovered from MPO$^{-/-}$ CD11b$^+$ macrophages (increased NO) versus WT CD11b+ cells (Fig. 1*C*); and (*iv*) significant reduction in degradation of *N*-acetyl PSA in MPO$^{-/-}$ CD11b+ macrophages, despite the presence of increased NO (Fig. 1*D*).

Our data show that *N*-acetyl PSA, which lacks the free amino group required for PSA deamination, is processed to a smaller molecular species by ROSs; *N*-acetyl PSA is not processed by MPO-deficient macrophages but is readily processed by iNOS-deficient DCs. Similarly, dextran, which is widely used to study endocytosis and/or trafficking in APCs, is degraded within the endosome/lysosome by ROSs (Fig. S2). Taken together with our data on the deaminative degradation of PSA, these results indicate that carbohydrates can be processed by ROSs and/or RNSs through different mechanisms, depending on the structure of the particular carbohydrate. Clearly, free amino-containing carbohydrates are more susceptible to RNSs in APCs.

RNSs, including NO and nitroxyl, chemically degrade PSA through deamination. Under controlled conditions, a product that has been partially deaminated (e.g., PSA-NO) is obtained. Either prolonging treatment of PSA with NO or increasing the NO concentration results in formation of smaller degraded products. Similarly, a highly degraded molecule is created by treatment of PSA with one representative ROS—hydroxyl radical formed as a result of autooxidation of a reduced metal, Fe^{2+}—at an increased reactant concentration or for increased reaction periods (data not shown). However, processing of PSA and *N*-acetyl PSA in APCs apparently is finely controlled, and the predominant products (≈10 kDa) degraded by RNSs and/or ROSs are consistently produced.

To test whether the deaminative products can be presented to and activate T cells *in vitro* and *in vivo* in the absence of iNOS,

we purified the NO-derived product PSA-NO (≈16 kDa, Fig. S3*A*). In the absence of iNOS, only the deaminative product PSA-NO—but not native PSA—activates T cells *in vitro* and *in vivo*. It is interesting that iNOS$^{-/-}$ DCs express lower levels of cell-surface membrane proteins (e.g., MHCII, CD80, and CD86) than WT DCs (21). Despite the requirement for MHCII and CD86 expression in PSA activation of T cells, ≈16-kDa PSA-NO still induces more vigorous T cell responses in these cells than full-sized PSA does in WT DCs (Fig. 2*C*). It is possible that PSA-NO is more readily available for presentation because it requires no depolymerization. This concept is consistent with the report of increased release of interleukin 2 after presentation of a short MUC1 (tumor antigen) peptide by DCs (22).

Complex protein antigens and long synthetic peptides are expected to require intracellular processing before presentation on MHCII. Small peptides derived from some (but not all) antigens can directly bind to cell-surface MHCII molecules and be presented equally well by fixed and nonfixed APCs (23). We found that blockage of PSA-NO trafficking through the MHCII pathway in APCs eliminates T cell responses. Presentation of PSA-NO by APCs depends on HLA-DR (human) or I-A/I-E (mouse). These data indicate that depolymerized PSA (PSA-NO) is still presented through the MHCII pathway and thus that iNOS-deficient cells are defective in processing but not in presenting intact PSA. DCs fixed before addition of PSA-NO do not elicit a response (Fig. 3*D*); this result suggests that metabolically active DCs are required for PSA-NO trafficking and presentation.

NO has been shown to depolymerize several glycosaminoglycans through the deamination reaction, and it was proposed that HNO_2 and NO shared one common intermediate, the nitrosium cation (NO^+) (9, 10, 24). The nitrosium cation nitrosate free amino groups or *N*-sulfate groups. The nitrosation of amino groups or *N*-sulfate groups causes loss of nitrogen gas with a ring contraction of 2-amino-2-deoxy sugars to 2,5-anhydro sugars coupled to elimination of the aglycone (24). In addition, 4-amino-4-deoxy sugars are also amenable to the deamination reaction through a reaction sequence similar to 2-amino-2-deoxy sugars (25, 26). However, whether NO-mediated deamination of 4-amino sugars results in the cleavage of the glycosidic bonds depends on the glycosidic linkage of 4-amino-4-deoxy sugars in the carbohydrate polymers (25, 26). For example, the deamination of 4-amino groups of 2-linked 4-amino-4,6-deoxymannopyranosyl residues yields 2-linked rhamnopyranosyl and 2-linked 6-deoxyallofuranosyl residues, but the glycosidic linkages stay intact (25). In contrast, the deamination of 4-amino groups of 3-linked 2-acetamido-4-amino-2,4,6-trideoxygalactopyranosyl (AAT*p*) residues yields cleavage at both C-3 and C-1 of AAT*p*, as was studied in detail by Lindberg *et al.* (26). It was established that three possible deamination reactions on the free amino group at C-4 of the 3-linked D-AAT*p* residues could take place and that two of these three reactions (reactions 2 and 3) cause the breakage of glycosidic bond, with one (reaction 3) being the major reaction (Fig. S1).

PSA contains a 3-linked AAT*p* residue (Fig. S1), and this is the only sugar eligible for a deamination reaction leading to depolymerization of PSA. Because the deamination mechanism of 3-linked AAT*p* on carbohydrate polymers is well described in the literature (26), we did not carry out additional experiments to redefine deamination at the cleavage site of PSA. To find out whether NO-mediated deamination of PSA disrupts the zwitterionic nature of PSA, we carried out a series of experiments. We ran 1D NMRs (Fig. 4) of the partially deaminated product PSA-NO along with PSA and observed no detectable difference in their structures. These data suggested that deamination took place only at the cleavage sites (approximately at every 16th AAT*p* residue). Then, we performed *N*-acetylation of both PSA and PSA-NO to see whether we could incorporate acetyl groups into these sugars. A perfect incorporation of one acetyl group per one repeating unit of PSA-NO showed that all free amino groups (within our detection limit) were intact. In addition, after the *N*-acetylation, a change in the chemical shift of C-6 of the AAT*p* residue of PSA-NO (as in PSA) proved that *N*-acetylation took place on the C-4 of AAT*p*. Our structural characterization of the deamination product PSA-NO showed that PSA-NO shares the same chain structure with PSA—with most AAT*p* residues staying intact—a requirement for sustaining this molecule's zwitterionic nature and antigenicity (17).

This study demonstrates that *B. fragilis* PSA (≈130 kDa) induces NO production, which is responsible for the polysaccharide's depolymerization, and that the chemical mechanism underlying PSA depolymerization is deaminative cleavage of the molecule into products of ≈10–15 kDa that can bind to MHCII and be presented to the CD4$^+$ T cell receptor. In contrast, chemically preprocessed polysaccharide (≈10–15 kDa) bypasses this deaminative step as a requirement for presentation through the MHCII pathway. The chemical mechanism described herein complements the classic processing route for exogenous protein antigens, in which the generation of peptides depends on protease digestion and provides new insight into T cell-dependent carbohydrate processing.

Materials and Methods

Mice, Cells, and Monoclonal Antibodies. WT (C57BL/6J), iNOS$^{-/-}$ (B6.129P2-Nos2^{ptm1Lau}/J), and MPO$^{-/-}$ (B6.129 × 1-Mpo^{tm1Lus}/J) (The Jackson Laboratory) mice (male, 6–8 weeks old) were maintained as described in ref. 1.

Human mononuclear cells were separated from blood and mouse mononuclear cells (MNCs) were separated from spleens on Ficoll–Hypaque gradients. CD4$^+$ T cells were purified from MNCs by CD4 negative selection (R&D Systems). Mouse DCs or monocytes/macrophages were separated from MNCs through CD11c or CD11b positive selection (Miltenyi Biotec).

Monoclonal antibody to HLA-DQ (SPV-L3) was from NeoMarkers; mAbs to HLA-DR (L243), I-A/I-E (M5/114.15.2), and isotype controls mouse IgG2a (MG2a-53), mouse IgG3 (MG3–35), and rat IgG2b (RTK4530) were from Biolegend; and mAbs to HLA-A, -B, and -C (W6/32) and HLA-DP (B7/21) were from Leinco Technologies. All mAbs and isotype controls were free of azide.

PSA Purification, Radiolabeling, and *N*-Acetylation. PSA was purified from a mutant *B. fragilis* strain overexpressing PSA as described in refs. 4 and 27. The purity of PSA (lot 17, >99%) was assessed by SDS/PAGE, ^{1}H-NMR spectroscopy, and UV wavelength scans. PSA was radiolabeled by 20% oxidation of galactofuranose and reduction by ^{3}H-$NaBH_4$. The specific activity of ^{3}H-PSA was ≈2,800 cpm/ng. *N*-acetyl PSA was prepared by PSA treatment with acetic anhydride in 5% (wt/vol) $NaHCO_3$.

***In Vitro* Assays of Carbohydrate Processing in APCs.** To allow uptake and processing, a modified procedure (1) was used, with incubation of 100 μg of ^{3}H-PSA or ^{3}H-*N*-acetyl PSA together with 500 μg of unlabeled PSA (used to stimulate iNOS expression) for 72 h at 37°C with ≈3 × 10^6 CD11c splenic DCs from either WT or iNOS$^{-/-}$ mice; ≈7 × 10^6 CD11b+ monocytes/macrophages from spleens of WT or MPO$^{-/-}$mice were similarly treated. Cells were harvested, washed three times with PBS, suspended in 10 mM Tris·HCl, and digested directly with papain (0.4 mg/ml) at 37°C for 3 h and, subsequently, with pronase (0.2 mg/ml) overnight. For degradation of dextran, 1/4 μCi ^{3}H-dextran (≈70 kDa) (American Radiolabeled Chemicals) was incubated in ≈1 × 10^8 Raji cells for 18 h either alone or in the presence of 0.5 mM MnTBAP, 1 mM pyruvate, or 10 mM D-mannitol. Endosomal lysates were obtained as described in ref. 1.

RT-PCR. Splenic DCs (1 × 10^6/ml) were incubated with PSA (100 μg/ml) or lipopolysaccharide (LPS) (*Escherichia coli* K-235, 100 ng/ml; Sigma–Aldrich) for 18 h. Total RNA was extracted with an RNeasy kit (Qiagen), and purified RNA was used for RT-PCR with the SuperScript III One-Step RT-PCR System (Invitrogen). Primers (Operon Biotechnologies) used to amplify the cDNA of GAPDH (product size, 450 bp) were 5′-GGTGCTGAGTATGTCGTGGA-3′ and 5′-CACATTGGGGGTAGGAACAC-3′; iNOS primers were 5′-TCATGGACCACCACACAGCC-3′ and 5′-CGGATCTCTCTCCTCCTGGG-3′. The iNOS primers were designed to amplify a 244-bp product of cDNA codified within a region of the iNOS gene that was not included in the target construct and was absent in

iNOS$^{-/-}$ mice (28). The RT-PCR products and a 1-kb DNA ladder were run on 3% agarose gel and visualized with ethidium bromide.

NO Detection. WT or iNOS$^{-/-}$ splenic DCs (≈3 × 10^6/ml) with PSA (500 μg/ml) or LPS (1 μg/ml) were stimulated for 72 h. Nitrite production in the cell supernatants was measured with the Griess Reagent System.

***In Vitro* T Cell Proliferation Assays.** Human T cell proliferation assays were conducted as described in refs. 17 and 27. In brief, 5 × 10^4 enriched CD4$^+$ T cells and 1 × 10^5 irradiated MNCs (≈3,300 rad) were cocultured in 200 μl of modified RPMI medium 1640 (American Type Culture Collection) supplemented with 10% FBS and 1% penicillin–streptomycin. SEA (10 ng/ml) was used as a positive control. On day 6, cells were pulsed with [^{3}H]thymidine and harvested 8 h later. Radioactive uptake was measured by liquid scintillation. In blocking experiments with human cells, colchicine (1 μM), brefeldin A (100 μg/ml), or mAbs (1.5 μg/ml) to HLA-A, -B, and -C; HLA-DR, -DQ, and -DP; and isotype controls (IgG2a and IgG3) were cocultured with cells 30 min before addition of PSA-NO (100 μg/ml).

For the mouse T cell proliferation assay, PSA (100 μg/ml), PSA-NO (20 μg/ml), and SEA (10 ng/ml) were added to the coculture of 1 × 10^5 irradiated DCs and 2 × 10^5 CD4$^+$ T cells (200 μl per well). For blocking experiments with mouse cells, colchicine (0.5 μM), brefeldin A (50 μg/ml), or mAb (1.5 μg/ml) to I-A/I-E and its isotype IgG2b were cocultured with cells 30 min before addition of PSA-NO (20 μg/ml). In fixation experiments, DCs were fixed with 2% formaldehyde in PBS at 4°C for 30 min, and fixed DCs were washed twice with cold PBS before coculture with CD4$^+$ T cells. After 4 days, T cell proliferation was assayed as above.

Mouse Model for Intraabdominal Abscess Formation. In an intraabdominal abscess model (1, 29), mice were injected i.p. with 1× PBS (control), PSA (50 μg), or PSA-NO (50 μg) mixed with sterile cecal contents (SCC). Animals were killed 6 days later and examined for abscess formation. Abscess data represent two experiments.

Statistical Analyses. Abscess induction differences between groups were evaluated by Fisher's exact test (Instat; GraphPad Software). Means from T cell proliferation assays were compared by unpaired *t* test.

ACKNOWLEDGMENTS. We thank Ms. Jaylyn Olivo and Ms. Julie McCoy for helpful editorial assistance and Drs. Sarkis K. Mazmanian and Rachel McLoughlin for reading this manuscript. This work was supported by National Institutes of Health/National Institute of Allergy and Infectious Diseases Grant RO1 AI039576 (to D.L.K.).

1. Cobb BA, Wang Q, Tzianabos AO, Kasper DL (2004) Polysaccharide processing and presentation by the MHCII pathway. *Cell* 117:677–687.
2. Comstock LE, Kasper DL (2006) Bacterial glycans: Key mediators of diverse host immune responses. *Cell* 126:847–850.
3. Chan WK, Law HK, Lin ZB, Lau YL, Chan GC (2007) Response of human dendritic cells to different immunomodulatory polysaccharides derived from mushroom and barley. *Int Immunol* 19:891–899.
4. Baumann H, Tzianabos AO, Brisson JR, Kasper DL, Jennings HJ (1992) Structural elucidation of two capsular polysaccharides from one strain of *Bacteroides fragilis* using high-resolution NMR spectroscopy. *Biochemistry* 31:4081–4089.
5. Mazmanian SK, Liu CH, Tzianabos AO, Kasper DL (2005) An immunomodulatory molecule of symbiotic bacteria directs maturation of the host immune system. *Cell* 122:107–118.
6. Wang Q, *et al.* (2006) A bacterial carbohydrate links innate and adaptive responses through Toll-like receptor 2. *J Exp Med* 203:2853–2863.
7. Kolios G, Valatas V, Ward SG (2004) Nitric oxide in inflammatory bowel disease: A universal messenger in an unsolved puzzle. *Immunology* 113:427–437.
8. Brüne B (2005) The intimate relation between nitric oxide and superoxide in apoptosis and cell survival. *Antioxid Redox Signal* 7:497–507.
9. Hassan MS, Mileva MM, Dweck HS, Rosenfeld L (1998) Nitric Oxide products degrade chrondroitin sulfate. *Nitric Oxide* 2:360–365.
10. Vilar RE, *et al.* (1997) Nitric oxide degradation of heparin and heparan sulfate. *Biochem J* 324:473–479.
11. Kumar AP, Ryan C, Cordy V, Reynolds WF (2005) Inducible nitric oxide synthase expression is inhibited by myeloperoxidase. *Nitric Oxide* 13:42–53.
12. Li M, Rosenfeld L, Vilar RE, Cowman MK (1997) Degradation of hyaluronan by peroxynitrite. *Arch Biochem Biophys* 341:245–250.
13. Wong SF, Halliwell B, Richmond R, Skowreneck WR (1981) The role of superoxide and hydroxyl radicals in the degradation of hyaluronic acid induced by metal ions and by ascorbic acid. *J Inorg Biochem* 14:127–134.
14. Wink DA, *et al.* (1998) The cytotoxicity of nitroxyl: Possible implications for the pathophysiological role of NO. *Arch Biochem Biophys* 351:66–74.
15. Miranda KM, *et al.* (2005) Mechanism of aerobic decomposition of Angeli's salt (sodium trioxodinitrate) at physiological pH. *J Am Chem Soc* 127:722–731.
16. Vig M, *et al.* (2004) Inducible nitric oxide synthase in T cells regulates T cell death and immune memory. *J Clin Invest* 113:1734–1742.
17. Tzianabos AO, *et al.* (2000) T cells activated by zwitterionic molecules prevent abscesses induced by pathogenic bacteria. *J Bio Chem* 275:6733–6740.
18. Prigozy TI, *et al.* (2001) Glycolipid antigen processing for presentation by CD1d molecules. *Science* 291:664–667.
19. Mani K, Cheng F, Fransson LA (2007) Heparan sulfate degradation products can associate with oxidized proteins and proteasomes. *J Biol Chem* 282:21934–21944.
20. Kaufmann SH, Schaible UE (2005) Antigen presentation and recognition in bacterial infections. *Curr Opin Immunol* 17:79–87.
21. Wong SH, Santambrogio L, Strominger JL (2004) Caspases and nitric oxide broadly regulate dendritic cell maturation and surface expression of class II MHC proteins. *Proc Natl Acad Sci USA* 101(51):17783–17788.
22. Vlad AM, *et al.* (2002) Complex carbohydrates are not removed during Processing of glycoproteins by dendritic cells: Processing of tumor antigen MUC1 glycopeptides for presentation to major histocompatibility complex class II-restricted T cells. *J Exp Med* 196:1435–1446.
23. Ceppellini R, *et al.* (1989) Binding of labelled influenza matrix peptide to HLA DR in living B lymphoid cells. *Nature* 339:392–394.
24. Shively JE, Conrad HE (1976) Formation of anhydrosugars in the chemical depolymerization of heparin. *Biochemistry* 15:3932–3942.
25. Kenne L, Lindberg B, Unger P, Gustafsson B, Holme T (1982) Structural studies of the *Vibrio cholerae* O-antigen. *Carbohydr Res* 100:341–349.
26. Lindberg B, Lindqvist B, Lonngren J, Powell DA (1980) Structural studies of the capsular polysaccharide from *Streptococcus pneumoniae* type 1. *Carbohydr Res* 78:111–117.
27. Kalka-Moll WM, *et al.* (2002) Zwitterionic polysaccharides stimulate T cells by MHC class II-dependent interactions. *J Immunol* 169:6149–6153.
28. Gomez-Ambrosi J, *et al.* (2004) Reduced adipose tissue mass and hypoleptinemia in iNOS deficient mice: Effect of LPS on plasma leptin and adiponectin concentrations. *FEBS Lett* 577:351–356.
29. Chung DR, *et al.* (2002) CD4+ T cells regulate surgical and postinfectious adhesion formation. *J Exp Med* 195:1471–1478.